IEEE Sensor Letters

by Syah Alam FTI

Submission date: 17-Apr-2025 04:42PM (UTC+0700)
Submission ID: 2228863216
File name: 2_Final_Manuscript_Clear_SENSL-24-12-RL-0183.R1_Clear.docx (1.11M)
Word count: 2973
Character count: 16017

IEEE Sensors Letters Volume 2(3) (2017)
Microwave/millimeter wave sensors

Collaboratively Far-Field and Near-Field Regions for Dual-Modalities Microwave Permittivity Sensor using T-Shaped Resonator Embedded with IDC

Syah Alam[1*], Zahriladha Zakaria[2**], Indra Surjati[1*], Noor Azwan Shairi[2*], Mudrik Alaydrus[3**], Teguh Firmansyah[4*], Yuli Kurnia Ningsih[1*], Lydia Sari[1*]

[1] Department of Electrical Engineering, Universitas Trisakti, DKI Jakarta, 11440
[2] Faculty of Electronic and Computer Technology and Engineering, Universiti Teknikal Malaysia Melaka (UTeM), Malaysia
[3] Department of Electrical Engineering, Universitas Mercu Buana, West Jakarta 11650, Indonesia.
[4] Department of Electrical Engineering, Universitas Sultan Ageng Tirtayasa, Kota Serang, Banten 42124, Indonesia.
* Member, IEEE
** Senior Member, IEEE

Received 1 Nov 2016, revised 25 Nov 2016, accepted 30 Nov 2016, published 5 Dec 2016, current version 15 Dec 2016. (Dates will be inserted by IEEE; "published" is the date the accepted preprint is posted on IEEE Xplore®; "current version" is the date the typeset version is posted on Xplore®).

Abstract—This letter introduces collaboratively far-field and near-field regions for dual modalities permittivity sensor to characterized solid materials. The proposed sensor comprises a T-shaped resonator featuring a single port embedded with Interdigital capacitor (IDC). The 1st resonator, operating at f_{r1} = 2.43 GHz as the long-distance detection utilizes the far field region, while the 2nd resonator, working at f_{r2} = 1.64 GHz, functions as the contact detection utilizes the near field region. These resonators possess distinct sensing hotspots, enabling independent utilization. Contact detection is achieved by utilized the near-field region by placing the material under test (MUT) directly above the surface of the 2nd resonator, while the 1st resonator for long-distance detection utilized the far-field region by using the interrogator antenna at a distance of d = 10 cm. The experimental results demonstrate that the proposed sensors exhibit a maximum sensitivity of 5.13% and 3.40% for near field and far field detection, respectively. Moreover, the average accuracy for both contact and long-distance detection is 95.99% and 95.16%, respectively, when compared to the permittivity values obtained from the datasheet within the range of 1 - 6.15. This research holds significant practical value for the contact and long-distance characterization of solid materials, particularly in applications such as biomedical, quality control, and pharmaceutical industries.

Index Terms—microwave sensor, dual modalities, near-field, far-field, solid materials

I. INTRODUCTION

Microwave sensors (MS) have gained widespread development for assessing both solids and liquids due to their benefits, including high precision, a high Q-Factor, affordability, and compact size[1]. One of the properties they can detect is permittivity, which refers to a material's capacity to retain an electric field. Moreover, permittivity of the MUT can be ascertained through perturbation theory, assuming the MUT acts as a capacitive load [2]. Previous studies have put forth various microwave sensors employing resonators such as Split Ring Resonator (SRR)[3], Complementary Split Ring Resonator (CSRR) [4], Substrate Integrated Waveguide (SIW) [5], and Interdigital Capacitor (IDC) [6] for assessing solid substances. In contrast, previous work proposed by [7] introduces a dual T-shaped resonator featuring a single port for characterizing solid materials with contact and non-contact. However, this work has disadvantages such as a very limited distance of 0.5 - 1.5 mm for non-contact detection, poor sensitivity and the locations of the E-field and H-field are ambiguous. Another work, presented by [8], suggests a multifunctional dual-band MS with an antenna for communication purposes. However, the MUT's characterization is only performed directly by placing it on the sensing hotspot. Additionally, [9] and [10] employs an antenna as a permittivity sensor for contactless detection at a distance of 20 mm and 30 mm using Artificial Magnetic Conductor (AMC) . However, the proposed sensor features only one sensing hotspot and therefore cannot facilitate contact and long-distance characterization independently. Therefore, several requirements are needed to obtain high performance MS with long-distance detection, high sensitivity, clear location between E-field and H-field and dual hotspot location for contact and long-distance.

To fulfill this requirement, this letter introduces a collaboration between near-field and far-field regions for microwave permittivity sensors operating at two resonant frequencies. In detail, the main contribution of this research such as proposed long-distance detection MS with two independent sensing hotspots enabling contact and long-distance characterization of solid materials. To obtain a clear location

Corresponding author: Syah Alam (syah.alam@trisakti.ac.id). If some authors contributed equally, write here, "F. A. Author and S. B. Author contributed equally."

IEEE Sensors Letters discourages courtesy authorship; please use the Acknowledgment section to thank your colleagues for routine contributions.
Digital Object Identifier: 10.1109/LSEN.XXXX.XXXXXXX (inserted by IEEE).

between E-field and H-field with high sensitivity performance, a T-shaped resonator embedded with interdigital capacitors (IDC) was proposed. The 1st resonator operating at f_{r1} = 2.43 GHz for long-distance detection and the 2nd resonator operating at f_{r2} = 1.64 GHz for contact detection. Furthermore, near-field and far-field regions for permittivity detection are determined based on S_{11} and the radiation pattern of the two resonators while for distance of *(d)* refer to Fresnel region with $d \geq \frac{2D^2}{\lambda}$ [11].

II. SENSOR DESIGN

A. Scenario of near-field and far field region for characterization of solid materials

In this letter, two scenarios are proposed for far-field and near-field region characterization of solid materials using the proposed sensor as shown in **Fig. 1(a)** and **Fig. 1(b)** with the following explanation:

1) Furthermore, scenario (1) proposes long-distance detection using interrogator antennas operating at the same resonance frequency as the 1st resonator at f_{r1}= 2.32 GHz with $S_{11} \leq$ -10 dB and separated by distance (d) of 10 cm. Long-distance permittivity detection is carried out by observing changes in the resonant frequency based on S_{21} as shown in **Fig. 1(a)**.
2) For scenario (2), near-field region for contact detection is proposed by placing the MUT on the IDC of the 2nd resonator operating at f_{r2}= 1.52 GHz with $S_{11} \geq$ -10 dB by observing changes in the resonant frequency based on S_{11} as shown in **Fig. 1(b)**.

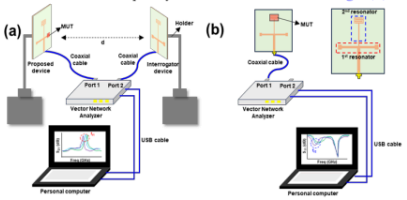

Fig. 1. Scenario of permittivity detection using proposed sensor; (a) scenario (1) for long-distance detection using an interrogator antenna, (b) scenario (2) for contact detection

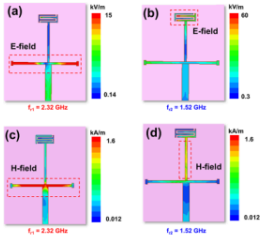

Fig.2 (a) E-field at f_{r1}, (b) E-field at f_{r2}, (c) H-field at f_{r1} (d) H-field at f_{r2}

The location of the sensing hotspot is determined based on the concentration of the E-field and H-field of the proposed resonator. The surface of the resonator with high E-field can be used to detect the permittivity of MUT. The E-field and H-field concentrations of the resonator are shown in **Fig. 2(a)**, **Fig. 2(b)**, **Fig. 2(c)** and **Fig. 2(d)**.

Fig. 2(a) and **Fig. 2(c)** show that the high E-field and H-field concentrations at f_{r1} = 2.32 GHz are at the same location on the arms of the 1st resonator. Other findings, **Fig. 2(b)** and **Fig. 2(d)** show that the highest E-field is in the gap of the IDC while the H-field is in the arm of the 2nd resonator. Furthermore, simulation of the radiation patterns at f_{r1} = 2.32 GHz and f_{r2} = 1.52 GHz are shown in **Fig.3 (a)**, **Fig.3 (b)** and **Fig. 3 (c)**.

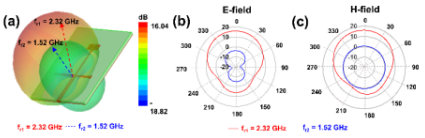

Fig.3 Radiation pattern of proposed resonator at f_{r1} = 2.32 GHz and f_{r2} =1.52 GHz, (b) E-field at f_{r1} = 2.32 GHz and f_{r2} =1.52 GHz, (c) H-field at f_{r1} = 2.32 GHz and f_{r2} =1.52 GHz.

Fig.3 (a) shows that the radiation pattern at f_{r1} = 2.32 GHz is higher than f_{r2} = 1.52 GHz. This finding is also in line with the simulations of E-field and H-field radiation shown in **Fig. 3 (b)** and **Fig. 3 (c)**. This shows that resonators with high radiation can be used for long-distance detection by utilizing the far-field region, while low radiation can be used for contact detection by utilizing the near-field region.

B. Structure of proposed sensor

The dual modalities sensor is constructed utilizing of FR-4 substrate with specific properties: a dielectric constant (ε_r) of 4.3, a loss tangent (tan δ) of 0.0265, and a thickness (h) of 1.6 mm.

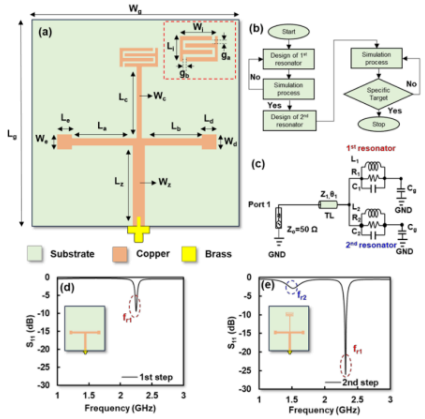

Fig. 4. (a) Structure of T-shaped resonator, (b) flowchart of design process, (c) equivalent circuit, (d) 1st step model, (e) 2nd step model.

The configuration of T-shaped resonator and IDC can be observed in **Fig.4 (a)**. Detailed dimensions of the proposed T-shaped resonator can be described as follows W_c = 3 mm, L_c = 17 mm, L_a = 16 mm, L_b = 12.5 mm, L_c = 18 mm, L_d = L_e = 1 mm, W_d = W_e = 2 mm, W_g = L_g 50 mm while for IDC represented by W_f = 9.5 mm, L_f = 3.5 mm and g_a = g_b = 1 mm. Moreover, the flowchart of design process dual T-shaped resonator is presented in **Fig.4 (b)** while for equivalent circuit shown in **Fig 4 (c)**. In the initial phase, the resonator functions at f_{r1} = 2.32 GHz as shown in **Fig.4 (d)**, while in the subsequent phase, it operates at a dual-band resonant frequency, with f_{r1} = 2.32 GHz and f_{r2} = 1.52 GHz as shown in **Fig.4 (e)**, respectively.

III. MEASUREMENT AND VALIDATION

A. Measurement of proposed sensor

Furthermore, **Fig.5(a)** demonstrates that the measurement setup while the outcomes are consistent and exhibit dual-band characteristics in accordance with the simulated results as shown in **Fig.5 (b)**. Nonetheless, there is a slight deviation in the resonant frequencies of the resonator. Specifically, f_{r1} shifts from 2.32 GHz to 2.43 GHz, with S_{11} of -15.05 dB, and f_{r2} shifts from 1.52 GHz to 1.64 GHz, with S_{11} of -3.01 dB. This discrepancy can be attributed to minor variations in the fabrication process and inherent fluctuations in the permittivity of the FR-4 substrate, ranging from 3.8 to 4.8[12].

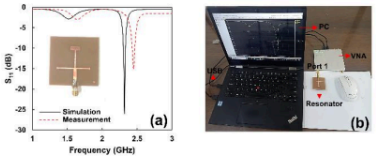

Fig. 5. (a) Comparison simulation and measurement result of proposed resonator, (b) measurement setup of proposed resonator

B. Experimental validation

The experimental validation was conducted utilizing a Vector Network Analyzer (VNA) spanning a frequency range of 1 - 3 GHz, with a frequency sweep increment of 0.01 GHz. The ambient temperature during the measurements was maintained at 25°C. Additionally, four distinct materials with known permittivity were employed as Material Under Test (MUT): RO5880 possessing a permittivity of 2.20, RO4003 of 3.65, FR-4 of 4.30, and RO3006 of 6.15 with the dimension of MUT is 10 x 10 x 1.6 mm^3. Moreover, to ensure the location of the MUT is constant we carefully place the MUT at the location of the sensing hotspot using plastic clamp which is for contact detection on the surface of the IDC and for long-distance detection on the surface of the T-shaped resonator as shown in **Fig 6 (b)** and **Fig 6(a)**. Furthermore, **Fig.7 (a)** shows that f_{r1} shifts to low frequency in line with the increased permittivity of the MUT placed at the sensing hotspot of the 1st resonator for long-distance detection with d = 10 cm while f_{r2} is fixed. The resonant frequency of the 1st resonator shifted from 2.43 GHz to 2.35 GHz with a permittivity range of 1 - 6.15 as shown in **Fig.7 (c)**.

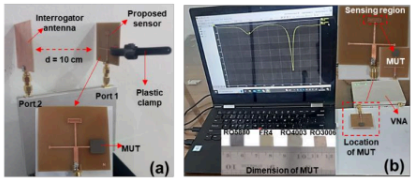

Fig. 6. Measurement setup; (a) long-distance detection using scenario (1), (b) contact detection using scenario (2).

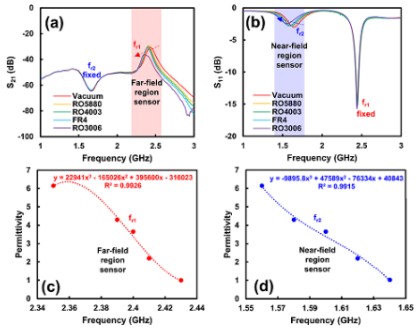

Fig. 7. Permittivity detection using proposed sensor, (a) long-distance detection with d = 10 cm, (b) contact detection, (c) polynomial equation for long-distance detection, (d) polynomial equation for contact detection.

In the other hand, **Fig. 7 (b)** shows the performance of the proposed sensor for contact detection. It is evident that f_{r2} experiences a downward shift in resonant frequency, corresponding to the increased permittivity of the MUT positioned on the sensing hotspot of the 2nd resonator, whereas f_{r1} remains constant. Moreover, **Fig. 7 (d)** shows that f_{r1} shifted to the lower frequency from 1.64 GHz to 1.56 GHz in line with the increased permittivity of the MUT placed on the 1st resonator while f_{r2} was fixed for permittivity range of 1 – 6.15.

C. Sensitivity and accuracy of proposed sensor

The sensitivity of the microwave sensor is determined from the shift in the resonant frequency when the MUT is placed on the sensing hotspot. The frequency shift is represented as Δf which shows the difference between the loaded and unloaded frequencies of the resonator. The frequency shift (Δf), sensitivity (S) and Frequency Detection Resolution (FDR) of the microwave sensor can be determined using the following **Eq. (1)**, **Eq. (2)** **and** **Eq. (3)**[13][14]:

$$\Delta f = (f_{\ unloaded} - f_{\ loaded})\ GHz \quad (1)$$

$$S = \left(\frac{f_{unloaded} - f_{loaded}}{f_{unloaded}}\right)\% \quad (2)$$

$$FDR = \frac{\Delta F}{\Delta \varepsilon_r} \quad (3)$$

TABLE 2. Comparison with previous work

Ref	f_r (GHz)	Range of ε_r	Dimension (mm)		Num. of sensing hotspot	d (mm)	FDR (GHz)	S (%) / Q-factor	Separated E & H field	Contact / long-distance detection
			Sensor	Sample						
[7]	1.81/2.34	1 – 6.15	50 x 50	10 x 10 x 1.6	2	1.5	0.023/0.003	2.30 /117	No	Yes / No
[8]	1.50/2.00/2.45	1 – 6.15	50 x 50	10 x 10 x 1.6	2	0.0	0.013/0.027	2.71 /120	No	Yes / No
[9]	6.90	1 – 15	40 x 40	10 x 10 x 4	1	20	0.038	3.80 /69	No	No / Yes
[10]	4.04	2 – 4	30 x 30	25 x 25 x 2.1	1	30	NA	1.89 /268	No	No / Yes
T.W.	1.64/2.43	1 – 6.15	50 x 50	10 x 10 x 1.6	2	100	0.016/0.016	5.13 /121	Yes	Yes / Yes

where Δf represents frequency shift in GHz, S represents the sensitivity of the sensor in percentage, $f_{unloaded}$ represent the resonance frequency of the resonator before being loaded by the MUT and f_{loaded} the frequency of the resonator when it is loaded with an MUT. In this letter, the $f_{unloaded}$ used is when the resonator with permittivity of vacuum $\varepsilon_r = 1$. Based on calculations using **Eq. (1)** and **Eq. (2)** shows that the maximum Δf of the 1st resonator and 2nd resonator has the same value of 0.08 GHz /$\Delta\varepsilon_r$ while the average sensitivities are 1.43% and 2.53%, respectively. The permittivity of the MUT is extracted using a polynomial equation obtained from the shift in the resonant frequency of the resonator as shown in **Fig.7(b)** and **Fig.7 (d)**. Therefore, the permittivity of the MUT for both detections can be determined using **Eq. (4)** and **Eq. (5)** as follows:

$$\varepsilon_{r1} = 22941 f_{r1}^{\,3} - 165026\, f_{r1}^{\,2} + 395600 f_{r1} - 316023 \quad (4)$$

$$\varepsilon_{r2} = -9895.8 f_{r2}^{\,3} + 47589\, f_{r2}^{\,2} - 76334 f_{r2} + 40843 \quad (5)$$

where f_{r1} is the resonant frequency of the 1st resonator and ε_{r1} is the permittivity of the MUT used for long-distance detection while f_{r2} is the resonant frequency of the 2nd resonator and ε_{r2} is the permittivity of the MUT used for contact detection. The overall performance of the proposed sensors both for long-distance and contact detection are shown in **Table 1**.

TABLE 1. Performance of proposed sensor

MUT	ε_r ref	Δf (GHz / $\Delta\varepsilon_r$)		Sensitivity (%)		Accuracy (%)	
		f_{r1}	f_{r2}	f_{r1}	f_{r2}	f_{r1}	f_{r2}
Vacuum	1.00	0	0	-	-	97.91	95.64
RO5880	2.20	0.02	0.02	0.83	1.23	92.38	92.08
RO4003	3.65	0.03	0.04	1.25	2.50	92.65	92.84
FR4	4.30	0.04	0.06	1.67	3.80	97.08	95.95
RO3006	6.15	0.08	0.08	3.40	5.13	99.93	99.29

Moreover, FDR of the proposed sensor based on **Eq. (3)** for f_{r1} and f_{r2} are 0.016 GHz. **Table 2** shows that the MS has novel dual modalities for contact and long-distance detection by utilizing the near-field and far-field region with a high sensitivity of 5.13%, long-distance detection with d = 100 mm and maximum Q-factor of 121 for solid materials with a permittivity range of 1 - 6.15 and two different sensing hotspots compared with previous work which only supports contact or long-distance detection and limited distance for long-distance detection.

IV. CONCLUSION

In this letter, dual modalities microwave sensor for long-distance and contact detection by utilizing the far-field and near-field region has been successfully designed and realized. The MS consists of T-shaped resonators embedded with IDC operating at f_{r1} = 2.43 GHz and f_{r2} = 1.64 GHz with different sensing hotspots and have independent characteristics. From the measurement results, a maximum sensitivity of 3.40% and 5.13% was obtained for long-distance detection using the interrogator antenna with a distance (d) = 10 cm and contact detection. Furthermore, the average accuracy of 1st and 2nd resonator is 95.99% and 95.16%, respectively. The proposed sensor can be a promising solution and can be recommended for contact and long-distance characterization of solid materials for biomedical, pharmaceutical, and quality control industries.

REFERENCES

[1] K. S. L. Parvathi and S. R. Gupta, "Ultrahigh-Sensitivity and Compact EBG-Based Microwave Sensor for Liquid Characterization," *IEEE Sensors Lett.*, vol. 6, no. 4, pp. 19–22, 2022, doi: 10.1109/LSENS.2022.3159800.

[2] A. Aquino, C. G. Juan, B. Potelon, and C. Quendo, "Dielectric Permittivity Sensor Based on Planar Open-Loop Resonator," *IEEE Sensors Lett.*, vol. 5, no. 3, pp. 2021–2024, 2021, doi: 10.1109/LSENS.2021.3055544.

[3] S. Kiani, P. Rezaei, and M. Navaei, "Dual-sensing and dual-frequency microwave SRR sensor for liquid samples permittivity detection," *Meas. J. Int. Meas. Confed.*, vol. 160, p. 107805, 2020, doi: 10.1016/j.measurement.2020.107805.

[4] H. Xiao, S. Yan, C. Guo, and J. Chen, "Microwave / millimeter wave sensors A Dual-Scale CSRRs-Based Sensor for Dielectric Characterization," vol. 6, no. 12, pp. 10–13, 2022.

[5] W. Liu, J. Zhang, and K. Huang, "Wideband microwave interferometry sensor with improved sensitivity for measuring minute variations in dielectric properties of chemical liquids in microfluidic channels," *Meas. J. Int. Meas. Confed.*, vol. 189, no. September 2021, p. 110474, 2022, doi: 10.1016/j.measurement.2021.110474.

[6] S. Kiani, P. Rezaei, M. Navaei, and M. S. Abrishamian, "Microwave Sensor for Detection of Solid Material Permittivity in Single/Multilayer Samples With High Quality Factor," *IEEE Sens. J.*, vol. 18, no. 24, pp. 9971–9977, 2018, doi: 10.1109/JSEN.2018.2873544.

[7] S. Alam, Z. Zakaria, I. Surjati, N. A. Shairi, M. Alaydrus, and T. Firmansyah, "Integrated Microwave Sensor and Antenna Sensor Based on Dual T-Shaped Resonator Structures for Contact and Noncontact Characterization of Solid Material," *IEEE Sens. J.*, vol. 23, no. 12, pp. 13010–13018, 2023, doi: 10.1109/JSEN.2023.3273008.

[8] S. Alam, Z. Zakaria, I. Surjati, N. A. Shairi, M. Alaydrus, and T. Firmansyah, "Multifunctional of dual-band permittivity sensors with antenna using multicascode T-shaped resonators for simultaneous measurement of solid materials and data transfer capabilities," *Meas. J. Int. Meas. Confed.*, vol. 217, no. November 2022, p. 113078, 2023, doi: 10.1016/j.measurement.2023.113078.

[9] Q. Shi, X. W. Xuan, H. K. Nie, Z. Y. Wang, and W. Wang, "Antenna Sensor Based on AMC Array for Contactless Detection of Water and Ethanol in Oil," *IEEE Sens. J.*, vol. 21, no. 19, pp. 21503–21510, 2021, doi: 10.1109/JSEN.2021.3102294.

[10] W. J. Wu and G. Wang, "A modified AMC-based antenna sensor for long-distance measurement of complex permittivity," *Meas. J. Int. Meas. Confed.*, vol. 206, no. June 2022, p. 112261, 2023, doi: 10.1016/j.measurement.2022.112261.

[11] Pozar DM. *Microwave Engineering*. Fourth Edi. John Wiley & Sons, Inc; 2012

[12] A. Armghan, T. M. Alanazi, A. Altaf, and T. Haq, "Characterization of Dielectric Substrates Using Dual Band Microwave Sensor," *IEEE Access*, vol. 9, pp. 62779–62787, 2021, doi: 10.1109/ACCESS.2021.3075246.

[13] R. A. Alahnomi, Z. Zakaria, E. Ruslan, S. R. Ab Rashid, and A. A. Mohd Bahar, "High-Q sensor based on symmetrical split ring resonator with spurlines for solids material detection," *IEEE Sens. J.*, vol. 17, no. 9, pp. 2766–2775, 2017, doi: 10.1109/JSEN.2017.2682266.

[14] S. Kiani, P. Rezaei, and M. Fakhr, "Real-Time Measurement of Liquid Permittivity Through Label-Free Meandered Microwave Sensor," *IETE J. Res.*, 2023, doi: 10.1080/03772063.2023.2231875.

IEEE Sensor Letters

ORIGINALITY REPORT

14%	11%	12%	5%
SIMILARITY INDEX	INTERNET SOURCES	PUBLICATIONS	STUDENT PAPERS

PRIMARY SOURCES

1	Submitted to National Institute of Technology, Raipur Student Paper	3%
2	patents.justia.com Internet Source	2%
3	spiral.imperial.ac.uk Internet Source	2%
4	discovery.researcher.life Internet Source	1%
5	semarakilmu.com.my Internet Source	1%
6	O. Ayop, M. K. A. Rahim, N. A. Murad, N. A. Samsuri. "Dual band polarization insensitive and wide angle circular ring metamaterial absorber", The 8th European Conference on Antennas and Propagation (EuCAP 2014), 2014 Publication	1%
7	Tianyu Qi, Guohua Liu, Jianyuan Yu, Shuren Jiang. "A Quarter-Mode Substrate Integrated Waveguide Microwave Sensor Loaded with CCRR for Solid Material Measurement", IEEE Sensors Journal, 2023 Publication	1%
8	Nilesh Kumar Tiwari, Surya Prakash Singh, M Jaleel Akhtar. "Adulteration detection in petroleum products using directly loaded coupled-line-based metamaterial-inspired submersible microwave sensor", IET Science, Measurement & Technology, 2019	1%

Publication

9	ddd.uab.cat Internet Source	1 %
10	upcommons.upc.edu Internet Source	<1 %
11	Osman Ayop, Mohamad Kamal A. Rahim, Noor Asniza Murad, Noor Asmawati Samsuri, Farid Zubir, Huda A. Majid. "Dual-band metamaterial perfect absorber with nearly polarization-independent", Applied Physics A, 2016 Publication	<1 %
12	haghparast.info Internet Source	<1 %
13	Abu Hanif, Mohammad Lutful Hakim, Touhidul Alam, Badariah Bais et al. "Highly sensitive miniaturized labyrinth shape circular split ring resonator (LC-SRR) based microwave sensor for low permittivity characterization applications", Engineering Science and Technology, an International Journal, 2024 Publication	<1 %
14	Huifeng Zhai, Xiuwei Xuan, Zheng Chen, Mingji Li, Hongji Li. " High-Sensitivity and Wide-Range Antenna Sensor Based on EBG and SiO for Soil Water Content Monitoring ", IEEE Transactions on Instrumentation and Measurement, 2023 Publication	<1 %
15	Yordan Garbatov, C. Guedes Soares. "Innovation in the Analysis and Design of Marine Structures", CRC Press, 2025 Publication	<1 %

Exclude quotes Off Exclude matches < 10 words

Exclude bibliography On